

(4/21/05)

## **Optical Pumping of Rubidium**

Advanced Laboratory, Physics 407  
University of Wisconsin  
Madison, WI 53706

### **Abstract**

A Rubidium high-frequency lamp is used as the pumping light source to excite Rubidium atoms in a sample cell. The pumping source light is filtered to transmit the  $D_1$  Rb line and polarizers are used to produce circular polarization. The circular polarization pumping mechanism selectively repopulates the sample cell ground state Rb Zeeman hyperfine levels away from thermal equilibrium populations according to whether the pumping light is left or right circularly polarized. The sample cell is then irradiated using RF coils with the frequency of the hyperfine levels, changing the transparency of the sample cell Rb vapor. The change in sample transparency is measured as a function of RF frequency in a Silicon photodiode detector. This technique is used to determine the nuclear spin and magnetic moments of the  $\text{Rb}^{87}$  ( $I=3/2$ ) and  $\text{Rb}^{85}$  ( $I=5/2$ ) isotopes.

# Optical pumping of Rubidium

Dr. Johannes Recht and Dr. Werner Klein

**Optical pumping is a process used in high frequency spectroscopy which was developed by A. Kastler. It allows the spectroscopy of atomic energy states in an energy region which is not accessible by means of direct, optical observation. Kastler was awarded the Nobel Prize for Physics for this in 1966.**

Transitions are induced in a low density atomic vapour by means of high-frequency irradiation. These transitions can be detected through a change in the optical absorption which occurs during this process. With the help of high-frequency spectroscopy, it is possible to observe transitions between the Zeeman levels of hyperfine states in weak magnetic fields, where the spacing between neighbouring Zeeman states is less than  $10^{-8}$  eV.

When the levels of these states are known - the energies can be calculated with 1st order quantum mechanical perturbation calculation [1] - one also obtains a method for measuring weak magnetic fields with almost the same accuracy as that with which the irradiating frequency can be determined, i.e. with an accuracy of 1 in  $10^8$ .

In addition, this process allows the experimental observation of the anomalous Zeeman effect. It was considered appropriate to develop an easy-to-handle measuring system, at least for higher education establishments, if not for secondary school instruction as well.

## 1 Physical fundamentals

### 1.1 Energy level scheme

Rubidium is an alkali metal in the first main group of the periodic table. The low energy states of this element can be described very well using Paschen notation.

The rubidium atom consists of a spherically symmetrical atomic residue with orbital spin 0, and one optically-active electron with an orbital angular momentum 0, 1, 2... and an electron spin of 1/2. The line structure of the energy states is illustrated in Fig. 1. It is caused by the half-integral electron spin, which leads to a multiplicity of 2, i.e. a doublet system. The ground state is an S-state; the orbital angular momentum here is  $L=0$ . The spin-orbit coupling results in a total angular momentum quantum number  $J=1/2$ . Due to this coupling, the first excited level with  $L=1$  splits up into a  $^2P_{1/2}$  and a  $^2P_{3/2}$  state. Both states can be easily excited in a gas discharge.

During the transitions from the first excited states  $^2P_{1/2}$  and  $^2P_{3/2}$  into the ground state  $^2S_{1/2}$ , the doublet  $D_1$  and  $D_2$  characteristic of all alkali atoms is emitted. For rubidium, the wavelengths of the transitions are 794.8 nm ( $D_1$  line) and 780 nm ( $D_2$  line).

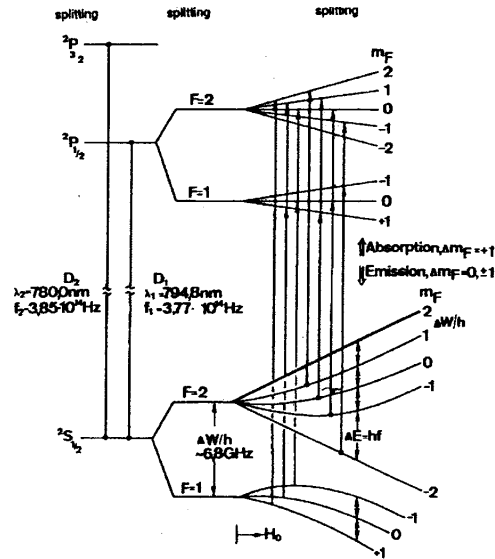


**Fig. 1 Energy Level Scheme for  $\text{Rb}^{87}$**

The hyperfine interaction, caused by the coupling of the orbital angular momentum  $J$  with the nuclear spin  $I$ , leads to the splitting of the ground state and the excited states. The additional coupling provides hyperfine levels with a total angular momentum  $F = I \pm J$ . For  $^{87}\text{Rb}$  with a nuclear spin  $I = 3/2$ , the ground state  $^2S_{1/2}$  and the first excited state  $^2P_{1/2}$  split up into two hyperfine levels with the quantum numbers  $F = 1$  and  $F = 2$ . Compared with the transition frequency of  $4 \times 10^{14} \text{ Hz}$  between  $^2P_{1/2}$  and  $^2S_{1/2}$ , the resulting splitting of the ground state and the excited states is much smaller. For the ground state, this hyperfine splitting of  $6.8 \times 10^9 \text{ Hz}$  is approx. 5 powers of 10 smaller than the fine structure splitting.

In the magnetic field, an additional Zeeman splitting (Fig. 1) into  $2F + 1$  sub-levels respectively is obtained. For magnetic fields of approx. 1 mT, the transition frequency between neighbouring Zeeman levels of a hyperfine state is  $8 \times 10^6 \text{ Hz}$ , i.e. another 3 powers of 10 smaller than the hyperfine splitting. The energy or frequency relationships between the individual states are of particular significance in understanding optical pumping.

## 1.2 Optical pumping

The process can be explained in more detail using the energy level scheme of  $^{87}\text{Rb}$  (Fig.1) as a reference. The transitions from  $^2S_{1/2}$  to  $^2P_{1/2}$  and  $^2P_{3/2}$  are electrical dipole transitions. They are only possible if the selection rules  $\Delta m_F = 0$  or  $\Delta m_F = \pm 1$  have been fulfilled.

The transitions between the Zeeman levels are detected using a method discovered by A. Kastler in 1950 which will be described in the following [1]. The  $D_1$  line emitted by the rubidium lamp displays such a high degree of Doppler broadening that it can be used to induce all permissible

transitions between the various Zeeman levels of the  $^2S_{1/2}$  and  $^2P_{1/2}$  states. If an absorption cell located in a weak magnetic field and filled with rubidium vapour is irradiated with the  $\sigma^+$  circularly-polarized component of the  $D_1$  line, the absorption taking place in the cell excites the various Zeeman levels which are higher by  $\Delta m_F = +1$ . However, the excited states decay spontaneously to the ground state and re-emit  $\pi$ ,  $\sigma^+$  or  $\sigma^-$  light in all spatial directions in accordance with the  $\Delta m_F = 0$  or  $\Delta m_F = \pm 1$  selection principle.

The irradiating, circularly-polarized light effects a polarization of the atomic vapour in the absorption cell. This can be interpreted as follows: during the process of absorption, the polarized light transmits angular momentum to the rubidium atoms. The rubidium vapour is polarized and thus magnetized macroscopically.

Without optical irradiation, the difference between the population numbers of the various Zeeman levels in the ground state is infinitesimally small, due to its low energy spacing in thermal equilibrium. However, the irradiation with  $\sigma^+$  light results in a strong deviation from the thermal equilibrium population. In other words, the population distribution changes as a result of optical pumping. The  $F=2$ ,  $m_F = +2$  level has the largest population probability - represented in Fig. 1 by bolder print - as the angular momentum selection principle prevents excitation from this level to higher ones. A Zeeman state with the  $m_F$  quantum number 3 does not exist in the first excited state. In other words, the irradiation of the absorption cell with the  $D_1$   $\sigma^+$  line generates a new population distribution in the equilibrium between optical pumping and the simultaneous relaxation processes. These are caused by depolarizing collisions of rubidium atoms with the walls of the vessel, or by interatomic collisions. In the pumping equilibrium, the population probabilities decrease in the order  $m_F = 2, 1, 0, -1, -2$  in the  $F=2$  state, and in the order  $m_F = -1, 0, +1$  in the  $F=1$  state.

In the case of the magnetic fields used here, the position of the energy states can be calculated with the Breit-Rabi formula [2]:

$$W(F, m_F) = -\frac{\Delta W}{2(2I+1)} - \mu_B g_I H_0 m_F \pm \frac{\Delta W}{2} \sqrt{1 + \frac{4m_F}{2I+1} x + x^2}$$

$$\text{with } x = \frac{g_J + g_I}{\Delta W} \mu_B H_0$$

$\Delta W$  = Hyperfine structure spacing

$g_J$  = g-factor of the orbital

$g_I$  = g-factor of the nucleus

The result is an average frequency spacing of approx. 8 MHz  $mT^{-1}$  between neighbouring Zeeman levels in the ground state  $^2S_{1/2}$  for  $^{87}\text{Rb}$ . This means that in a magnetic field of 1 mT, irradiation with a high frequency of 8 MHz can induce transitions between ground state levels. In the case of the magnetic fields used here, the energy spacing  $\Delta E_F = hf$  between the Zeeman levels in the ground state of  $^{87}\text{Rb}$  amounts to  $3 \times 10^{-8}$  eV. For the induced emission, the transition of the atom between two Zeeman levels with  $\Delta m_F = +1$  is accompanied by the emission of the

inducing HF quantum as well as one having the same energy. In view of the very small number of atoms available at a vapour pressure of  $10^{-5}$  mbar, the total energy released in this process is so low that a direct detection is not possible; a higher vapour pressure leads to a broadening of the lines due to collisions. If the HF field were observed directly, the signals would be masked entirely by noise. The process developed by A. Kastler requires that, for every act of induced emission, the population equilibrium between optical pumping and relaxation be changed by 1 atom. This allows the absorption of an additional pumping photon with an energy  $\Delta E_{\text{opt}} = 1.5$  eV. By observing this absorption directly, one thus achieves an amplification of  $1.5/(3 \times 10^{-8}) = 5 \times 10^7$ .

## 2 Experiment arrangement

Fig. 2 schematically illustrates the individual optical and magnetic components and the optical path.

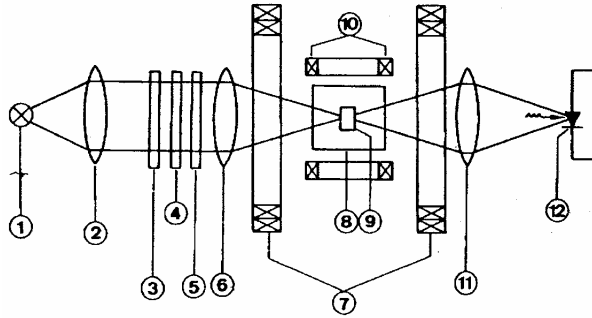


**Fig. 2 Schematic of the Experimental Setup**

A high-frequency rubidium lamp (1) serves as the light source. A quartz cell filled with 1 to 2 mbars of Argon and containing a small amount of rubidium is located in the electromagnetic field of a resonant circuit coil of an HF transmitter (60 MHz, 5W) which is integrated in the lamp housing. In order to prevent an excessive rate of rise of the Rb vapour pressure during HF excitation and thus the spontaneous inversion of the  $D_1$  line, the lamp temperature is maintained at approx 130 C by means of an electronically controlled thermostat. For this, the lamp is in thermal contact with the electrically heated base plate. A temperature sensor and a two-point controller in the supply device control the temperature of this plate and thereby the flow of heat between the lamp and the lamp housing. The lamp is located at the focus of the lens (2).

An interference filter (3), a linear-polarization filter (4) and a  $\lambda/4$  plate (5) are used to separate the  $\sigma^+$  circularly-polarized component of the  $D_1$  line from the emission spectrum of the rubidium lamp. The  $D_1$   $\sigma^+$  light thus generated is focused on to the absorption cell (9) with a lens (6) having a short focal length. The absorption cell (9) also contains rubidium. It is located in a water bath, the temperature of which is maintained at approx. 70 C with a circulation thermostat. At this temperature, the rubidium vapour pressure in the absorption cell settles at approx.  $10^{-5}$  mbar. The absorption chamber (8), together with the absorption cell (9) is located in a pair of Helmholtz coils (7), so that the magnetic field necessary for the Zeeman separation can be generated. The axis of the magnetic field coincides with the optical axis of the experiment set-up. The transmitted light is focused onto a silicon photodetector (12) by means of another lens (11)

with a short local length. The detector signal is proportional to the intensity of the radiation passing through the absorption cell and is fed to the Y input of an oscilloscope, an XY recorder or an interface, via a downstream current-to-voltage converter. HF coils (10) are positioned on both sides of the absorption cell. A function generator serves as the HF source. Its frequency is swept around by a gradually rising, saw-tooth voltage. This voltage is simultaneously used for the X-deflection of the registering system. As the HF coils are oriented perpendicularly with respect to the Helmholtz coil field, the linearly polarized HF coil field generates the circularly-polarized HF field necessary for the Zeeman transitions. The linearly polarized HF field can be divided into one right-handed and one left-handed circularly-polarized field; the component with the correct direction of rotation (corresponding to  $\Delta m_F = \pm 1$ ) induces transitions in the rubidium vapour of the absorption cell. This process makes it possible to observe the absorption in terms of its dependence on the HF irradiation.

### 3 Measurement Results

#### 3.1 Observation of the pump signal

Without HF irradiation, an equilibrium is reached in the absorption cell while pumping with  $\sigma^+$  light; in the ground state  $^2S_{1/2}$ ,  $F=2$ , the Zeeman level with  $m_F = +2$  is the most populated. The absorption of the cell is constant and thus so is the light intensity observed in transmission. If the circular polarization of the pumping light is now quickly changed from  $\sigma^+$  to  $\sigma^-$ , light is absorbed more strongly. With the irradiation from  $\sigma^-$  light, absorption transitions with  $\Delta m_F = -1$  are possible, and a new equilibrium settles in, where now the state  $^2S_{1/2}$ ,  $F = 2$ ,  $m_F = -2$  is the most populated. The circular polarization of the pumping light radiation ( $\sigma^+$  or  $\sigma^-$ ) relative to the magnetic field orientation is decisive in determining whether  $\Delta m_F = +1$  or  $\Delta m_F = -1$  transitions occur. Thus when right-handed circularly-polarized light is used for irradiation parallel to the magnetic field, it produces  $\Delta m_F = +1$  transitions, but for irradiation antiparallel to the field it causes  $\Delta m_F = -1$  transitions. Instead of the quick switchover from  $\sigma^+$  to  $\sigma^-$  pumping light, which is experimentally difficult to realize, a direction changeover of the magnetic field can be used. This change in the magnetic field direction can be easily carried out by changing the polarity of the Helmholtz coils with a switch. The signals observed when this is done (Fig. 3) are a clear indication that the absorption cell is being pumped optically.

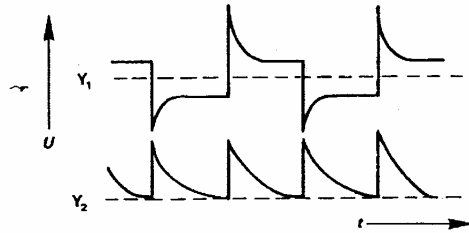


**Fig. 3** Above: Voltage Across the Helmholtz coil as a Function of Time  
Below: Pumping Light Signal as a Function of Time

#### 3.2 HF transitions between Zeeman levels in the ground state

Two processes can be used to observe the transitions between Zeeman levels in the ground state. In one case, the magnetic field can be slowly changed at constant frequency. With increasing magnetic field strength the energy spacing between neighbouring Zeeman levels increases. If this spacing is exactly  $E(F, m_F) - E(F, m_F-1) = hf_0$  and if  $f_0$  is the frequency of the irradiating high frequency, induced transitions between the corresponding Zeeman levels take place and the absorption for the pumping light changes. If the HF irradiation is strong enough, population equilibrium of the corresponding Zeeman levels is forced and, as a result, a deviation from pumping equilibrium.

In the other case, the frequency of the irradiating HF field can be slowly varied at constant magnetic field strength. Here, the absorption changes each time  $\Delta E = hf$  reaches the spacing between neighbouring Zeeman levels. We will make use of the latter method here.

The spacing between neighbouring Zeeman levels in the hyperfine state  $F = 2$  increases monotonically in the order  $m_F = +2$  to  $+1$ ,  $+1$  to  $0$ ,  $0$  to  $-1$ ,  $-1$  to  $-2$  and in the  $F=1$  state from  $m_F = -1$  to  $0$ ,  $0$  to  $+1$ . As a result of this, the individual absorption signals appear in the corresponding order with increasing frequency of the HF irradiation. The relative position between the absorption transitions of the  $F = 2$  state and those of the  $F = 1$  state is dependent on the strength of the applied magnetic field. The intensity of the absorption lines is determined by the population difference between the Zeeman levels involved each time. When  $\sigma^+$  light is used for pumping, the transition  $F = 2$ ,  $m_F = +2$  to  $+1$  appears with the greatest intensity (Fig. 4). Here we are dealing with a special case of the anomalous Zeeman effect. If the polarization is changed, i.e.  $\sigma^-$  light is radiated into the absorption cell instead of  $\sigma^+$  light, or the magnetic field direction of the Helmholtz coils is reversed while the polarization is retained, the transition  $F = 2$ ,  $m_F = -2$  to  $-1$  appears with the greatest intensity.

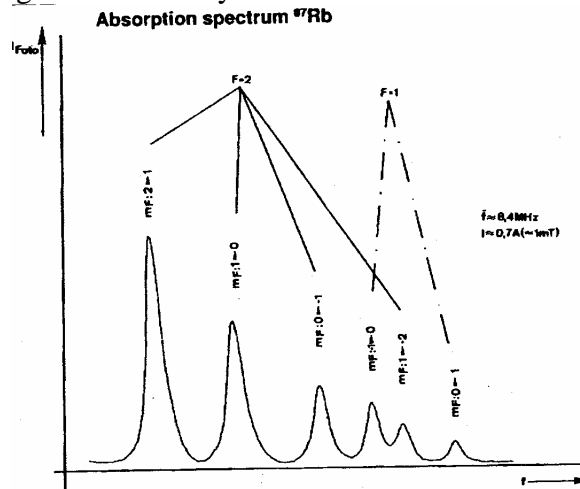


Fig. 4 Absorption Spectrum of  $\text{Rb}^{87}$  with  $\sigma^+$  Light

### 3.3 Zeeman splitting in $^{85}\text{Rb}$

A further special feature of the anomalous Zeeman effect is displayed in the multiplicity of the Zeeman energy levels in isotopes with different nuclear spins. In natural rubidium the isotopes  $^{87}\text{Rb}$  and  $^{85}\text{Rb}$  occur in the ratio 28: 72. While  $^{87}\text{Rb}$  has nuclear spin  $3/2$ ,  $^{85}\text{Rb}$  has a nuclear spin  $5/2$ . The corresponding angular momentum quantum numbers of the hyperfine levels are  $F = 3/2 + 1/2 = 2$  and  $F=3/2 - 1/2 = 1$  for  $^{87}\text{Rb}$  and  $F=3$  and  $F = 2$  for  $^{85}\text{Rb}$ . Due to the different nuclear g factors the hyperfine splitting is  $6.8 \times 10^9$  Hz for  $^{87}\text{Rb}$  and  $3.1 \times 10^9$  Hz for  $^{85}\text{Rb}$ .

This, however, means that for the same magnetic field the Zeeman splitting is of different magnitude for the two isotopes. While the splitting for  $^{87}\text{Rb}$  in the ground state has an average value of 8 MHz for a magnetic field of 1 mT, for  $^{85}\text{Rb}$  and the same field the corresponding value is 5 MHz.

Both pumping light source and absorption cell contain the natural isotope mixture. By setting the appropriate frequency on the function generator the Zeeman structures of the two isotopes can be observed separately. The hyperfine states with  $F = 2$  and  $F = 1$  for  $^{87}\text{Rb}$  split into  $2F + 1 = 5$  or  $2F + 1 = 3$  Zeeman levels respectively, while the splitting for  $^{85}\text{Rb}$  has 7 or 5 levels respectively. Correspondingly 4 + 2 lines occur in the  $^{87}\text{Rb}$  absorption spectrum (Fig. 5) and 6 + 4 lines in the  $^{85}\text{Rb}$  spectrum (Fig. 5).

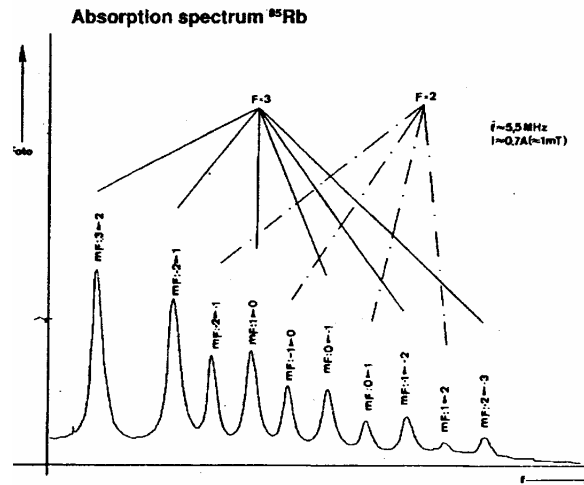


Fig. 5 Absorption Signal of  $\text{Rb}^{85}$  with  $\sigma^+$  Light

### 3.4 Multiple quantum transitions

Up to now, with the low HF field strength used, a single HF quantum has on each occasion caused the induced transition between directly neighbouring Zeeman levels. This situation changes when the HF field strength is increased. In addition to the normal single-quantum transitions which occur, we now have two-quanta transitions. In this case, the transition is induced by two HF quanta possessing half the transition energy in a primary action. The probability for such processes increases with the square of the HF field strength. For energy splitting between neighbouring levels corresponding to a transition frequency  $f$  and more intense HF irradiation at this frequency, transitions with  $\Delta m_F = 2$  are now possible. If the transitions  $F = 2$ ,  $m_F = +2$  to  $+1$  and  $m_F = +1$  to  $0$ , which appear at the transition frequencies  $f_1$  and  $f_2$  resp., are



observed, it can be seen that the two-quanta transition appears at the frequency  $(f_1 + f_2)/2$  with  $\Delta m_F = 2$ , i.e. at the geometric mean between  $f_1$  and  $f_2$ . These two-quanta transitions are distinguished by a very small half-width value of the absorption lines in comparison with that of the single-quantum transitions.

## Apparatus Settings

- Rb Lamp: Allow about 45 min for stable operation      Voltage = 18.5 V  
Temp = 110°
- Circulation Thermostat  
Temp = 65°
- Lenses: Require focus at center of Rb cell and at the Si photodiode detector.
- Line Filter: Shiny side should face the Rb lamp.
- Magnetic Field: About 12 gauss (740 mA)
- Function Generator  
Function: Sine  
Amplitude: Middle Position  
Attenuation: 20 dB  
DC-offset: 0  
Sweep Button: Pressed  
Mode: 'Cu  
Stop/Start: 8.5/7.5 MHz  
Period: about 500 ms (fast sweep)  
about 10 s (slow sweep)

## Procedure

- 1 Set up the Rubidium lamp as indicated above.
- 2 Check that the optics provides a focus at the Rb cell and the Si photodiode detector.
- 3 Set the polarizers to provide either  $\sigma^+$  or  $\sigma^-$  light.
- 4 Set the circulation thermostat to 65° and bring the sample Rb cell up to this temperature.
- 5 Set up the detector output on a scope and measure the signal level from the Rb lamp. The signal is a DC level and requires DC coupling on both the Pre Amp and scope.
- 6 Measure the optical pumping signal obtained by reversing the direction of the magnetic field. Do the same thing by changing the polarization of the excitation light. Check with the instructor that the size of your signal is reasonable. It may be necessary to change the settings of the lamp.
- 7 Set up the function generator for a frequency scan. Choose the magnetic field and start/stop frequencies based on the information provided in the tables below. Start with conditions appropriate for  $^{87}\text{Rb}$ . You may want to try several different frequencies and ranges to get an optimum signal. At this point you should be using the digital scope so that you can easily save the data. The scope should be set up in x-y mode with the sweep

output for x and the Pre Amp output for y. The Function Generator sweep output is on the back of the unit.

- 8 Do the same for  $^{85}\text{Rb}$ .

### **Analysis**

- 1 From the Breit-Rabi formula, derive an expression for the transition frequencies in terms of quantum numbers, magnetic moments, and the magnetic field.
- 2 Identify the lines you see in terms of their quantum number assignments. You may not see the lowest intensity lines until you optimize the scan conditions. Determine the nuclear spin of both isotopes based on the number of lines you see and lines which you think may be unobservable based on the expected relative intensities given below in the tables.
- 3 Determine the measured frequencies and compare to the expected values.
- 4 Calculate the Hyperfine Splitting for both  $\text{Rb}^{87}$  and  $\text{Rb}^{85}$  by solving the transition frequency expressions for  $\Delta W$  using your measured frequencies.

## Appendix A

### Properties of Rubidium

Properties-Nuclide	<sup>85</sup> Rb	<sup>87</sup> Rb
Nuclear Spin I	5/2	3/2
Nuclear Moment $\mu$	+1.35302	+2.7512
Gyromagnetic Ratio (rad T <sup>-1</sup> s <sup>-1</sup> )	2.5828 10 <sup>7</sup>	8.7532 10 <sup>7</sup>
Quadrupole Moment (m <sup>2</sup> )	0.25 10 <sup>-28</sup>	0.12 10 <sup>-28</sup>
Natural Abundance %	72.17	27.18
Half-Life T <sub>1/2</sub>	stable	stable
Hyperfine Splitting	3036 MHz	6835 MHz
D <sub>1</sub> = 794.8 nm		
D <sub>2</sub> = 780.0 nm		

## Appendix B

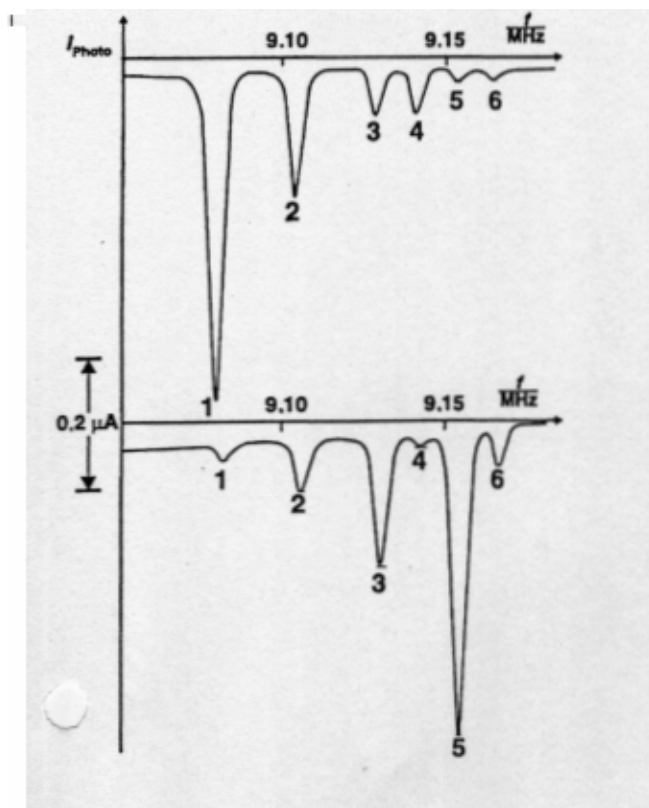
Transition frequencies and typical intensities for the Zeeman splitting of the two ground state hyperfine levels are shown below in Tables 1-4 for  $^{87}\text{Rb}$  and  $^{85}\text{Rb}$  at specific values of the magnetic field. This information can be used to plan your frequency sweeps.

**Table 1**  
 $^{87}\text{Rb}$  Transition Frequencies at  $B = 1.3031 \text{ mT}$

No.	f (MHz)	F	$m_F(1) \leftrightarrow m_F(2)$
1	9.080	2	$2 \leftrightarrow 1$
2	9.104	2	$1 \leftrightarrow 0$
3	9.128	2	$0 \leftrightarrow -1$
4	9.140	1	$1 \leftrightarrow 0$
5	9.153	2	$-1 \leftrightarrow -2$
6	9.165	1	$0 \leftrightarrow -1$

**Table 2**  
 $^{87}\text{Rb}$  Transition Intensities at  $B = 1.3031 \text{ mT}$

No.	$I(\sigma^+) \text{ mV}$	$I(\sigma^-) \text{ mV}$	$m_F(1) \leftrightarrow m_F(2)$
1	70	3	$2 \leftrightarrow 1$
2	26	10	$1 \leftrightarrow 0$
3	10	26	$0 \leftrightarrow -1$
5	3	70	$-1 \leftrightarrow -2$
4	9	3	$1 \leftrightarrow 0$
6	3	9	$0 \leftrightarrow -1$



**Absorption**  
 $\sigma^+$  Light (top) and  $\sigma^-$  Light (bottom)

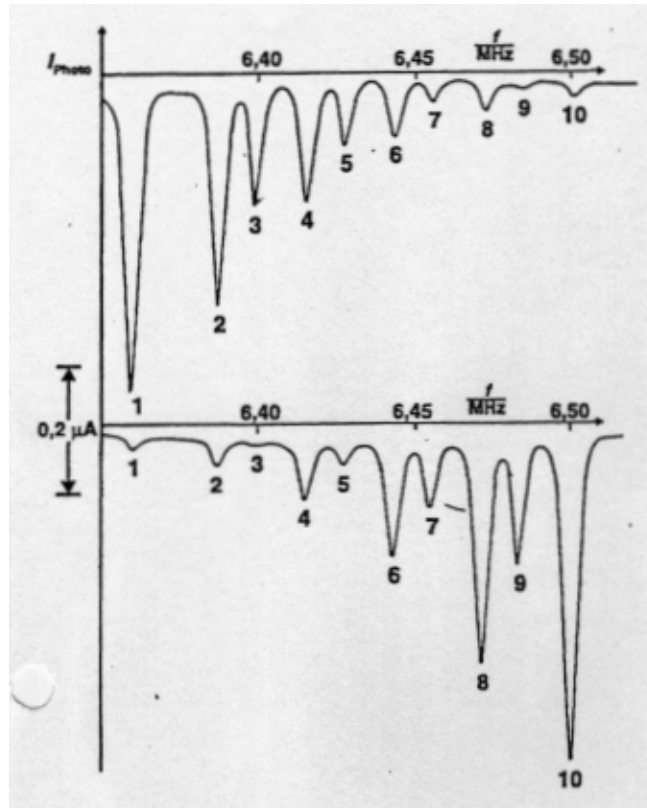
**Spectrum for  $^{87}\text{Rb}$  with**

**Table 3**  
<sup>85</sup>Rb Transition Frequencies at B = 1.3785 mT

No.	f (MHz)	F	m <sub>F</sub> (1) ↔ m <sub>F</sub> (2)
1	6.367	3	3 ↔ 2
2	6.394	3	2 ↔ 1
3	6.405	2	2 ↔ 1
4	6.420	3	1 ↔ 0
5	6.431	2	1 ↔ 0
6	6.447	3	0 ↔ -1
7	6.458	2	0 ↔ -1
8	6.474	3	-1 ↔ -2
9	6.486	2	-1 ↔ -2
10	6.502	3	-2 ↔ -3

**Table 4**  
<sup>85</sup>Rb Transition Intensities at B 1.3785 mT

No.	I(σ <sup>+</sup> ) mV	I(σ <sup>-</sup> )mV	m <sub>F</sub> (1) ↔ m <sub>F</sub> (2)
1	70	2	3 ↔ 2
2	43	5	2 ↔ 1
4	21	10	1 ↔ 0
6	10	21	0 ↔ -1
8	5	43	-1 ↔ -2
10	5	70	-2 ↔ -3
3	28	2	2 ↔ 1
5	13	5	1 ↔ 0
7	5	13	0 ↔ -1
9	2	28	-1 ↔ -2



Absorption Spectrum for <sup>85</sup>Rb with σ<sup>+</sup> Light (top) and σ<sup>-</sup> Light (bottom)